Plant Omics Journal POJ

POJ 4(5):270-277 (2011) ISSN:1836-3644

Defense proteins are induced in wheat spikes exposed to *Fusarium graminearum*

Kwang-Hyun Shin[1†], Abu Hena Mostafa Kamal[1†], Kun Cho[2], Jong-Soon Choi[3,4], Yu-Jin[1], Nam-Chon Paek[5], Yin Won Lee[6], Jong Kwan Lee[6], Jong-Chul Park[7], Heung-Tae Kim[8], Hwa-Young Heo[9]*, and Sun Hee Woo[1]*

[1]Department of Crop Science, Chungbuk National University, Cheong-ju 361-763, Korea
[2]Mass Spectrometry Research Center, Korea Basic Science Institute, Chungbuk 863-883, Korea
[3]Division of Life Science, Korea Basic Science Institute, Daejeon 305-333, Korea
[4]Graduate School of Analytical Science and Technology, Chungnam National University, Daejeon 305-764, Korea
[5]Department of Plant Science, Plant Genomics and Breeding Institute, and Research Institute for Agriculture and Life Sciences, Seoul National University, Seoul 151-921, Korea
[6]Department of Agricultural Biotechnology and Center for Fungal Pathogenesis, Seoul National University, Seoul 151-921, Korea
[7]Honam Agricultural Research Institute, National Institute of Crop Science, RDA, Iksan 570-080, Korea
[8]Department of Plant Medicine, Chungbuk National University, Cheong-ju 361-763, Korea
[9]Department of Plant Sciences and Plant Pathology, Montana State University, Montana 59717-3150, USA

†These authors are equally contributed to this work.
***Equally correspondence to: Sun-Hee Woo (shwoo@chungbuk.ac.kr) & Hwa-Young Heo (h.hwayoung@gmail.com)**

Abstract

Fusarium head blight (FHB), caused by *Fusarium graminearum*, infects wheat and barley and diminishes both grain yield and quality. *Triticum* spp. ecotypes differ in their susceptibility to this disease. Using a proteomics approach, we isolated and identified the proteins associated with FHB resistance in a popular Korean wheat genotype with moderate resistance. At 5 days post-anthesis, the floral spikes were point-inoculated with a macroconidial suspension of *F. graminearum*. After 48 h, we detected 31 of 100 acidic protein spots, and determined that these differentially expressed protein (DEP) spots were the result of FHB exposure. In all, 17 DEPs were up-regulated, 5 were down-regulated, and 2 were unevenly changed. Following tryptic digestion, we used MALDI-TOF/TOF mass spectrometry to identify 14 unique proteins in those 24 DEPs, including those related to carbon metabolism and photosynthesis. After inoculation, Rubisco small and large subunits, isoflavone reductase, a chloride carrier/channel, and (1,3;1,4) β-glucanase were markedly up-regulated, whereas wall-associated kinase 4 was down-regulated. In addition, a (1,3;1,4) β-glucanase protein (PR-2) was up-regulated in FHB-infected spikes, a finding that is in agreement with previous proteomics and transcriptomics analyses of other crops. Interestingly, most of these proteins were unevenly regulated over the course of infection, although their levels of protein expression were not lower than those untreated samples.

Keywords: *Fusarium graminearum*, *Fusarium* head blight, MALDI-TOF/TOF-MS, Rubisco, Scanning electron microscopy, Wheat.
Abbreviations: FHB_*Fusarium* head blight, MALDI_matrix assisted laser desorption/ionization, MS_mass spectrometry, SEM_scanning electron microscopy, TOF_time-of-flight.

Introduction

Plants counter pathogen invasions by activating a variety of defense mechanisms. Most species display resistance to such attacks through a combination of a general defense strategy and induced biochemical processes (Mahalingam et al., 2003). These responses may incorporate the reprogramming of cellular metabolism, accumulation of blockade substances, and the production of antimicrobial compounds that act directly to prevent invasion. Understanding the molecular mechanisms, these inducible defenses against fungal pathogens could be useful in designing protective strategies that would involve the expression of genes, encoding defense proteins in crop species. *Fusarium* head blight (FHB), or scab, causes by *Fusarium graminearum*. This devastating disease of wheat and other cereal grains is common in humid and semi-humid climates, causing a 30 to 50% loss in yield during epidemic years (McMullen et al., 1997). In particular, grains have poor quality and are contaminated with mycotoxins such as deoxynivalenol (DON), vomitoxin, and estrogenic zearalenone, all detrimental to humans and animals (Bai and Shaner, 2004). These mycotoxins have been implicated in pathogenesis, phytotoxicity, and the induction of apoptosis in eukaryotic cell cultures (Desjardins and Hohn, 1997; Kang and Buchenauer, 1999; Shifrin and Anderson, 1999). Host resistance is considered the most efficient means for controlling this disease (Martin and Johnston, 1982), and some germplasms have shown resistance activity against scab in wheat and other small grains that historically have hindered breeding efforts (Mesterházy, 1997). FHB resistance is classified into five types: initial infection, spread of infection, kernel infection, tolerance, and toxicity (van

Table 1. Quantitative distinctions in protein abundance from wheat spikes after 12, 24, or 48 h of treatment with *F. graminearum*.

Spot No.	12 HAI		24 HAI		48 HAI	
	Up/Down	Fold	Up/Down	Fold	Up/Down	Fold
Up-regulated						
4	↑	19.12	↑	13.86	↑	9.36
6	↑	14.04	↑	9.08	↑	1.26
7	↑	4.72	↑	5.51	↑	4.34
8	↑	1.30	↑	1.80	↑	1.66
9	↑	5.65	↑	4.38	↑	4.64
10	↑	6.20	↑	10.88	↑	9.06
11	↑	2.00	↑	1.54	↑	1.53
12	↑	6.09	↑	4.88	↑	5.47
13	↑	1.49	↑	1.97	↑	2.34
16	↑	4.99	↑	3.48	↑	1.61
17	↑	4.60	↑	5.08	↑	4.61
18	↑	1.12	↑	1.63	↑	1.62
19	↑	7.10	↑	9.10	↑	1.93
20	↑	3.93	↑	2.46	↑	1.81
21	↑	3.44	↑	1.64	↑	1.14
23	↑	51.22	↑	31.15	↑	30.60
31	↑	1.32	↑	2.59	↑	4.06
Down-regulated						
2	↓	4.66	↓	2.47	↓	4.30
5	↓	18.94	↓	2.95	↓	7.24
14	↓	6.46	↓	2.59	↓	4.04
29	↓	13.84	↓	1.95	↓	3.40
30	↓	1.57	↓	1.13	↓	3.06
Unevenly affected						
3	↓	0.15	↑	3.39	↑	3.56
22	↑	2.12	↑	1.32	↓	1.99

Eeuwijk et al., 1995). Genetic mapping results have implied that two or three major genes, together with various minor genes, control the initiation and spread of infection (Lin et al., 2004). Previous research has identified several host genes induced by *F. graminearum* exposure, and has determined which protein-encoding genes are up- or down-regulated in their expression (Pritsch et al., 2000; Kruger et al., 2002; Wang et al., 2005; Geddes et al., 2008; Taylor et al., 2008; Walter et al., 2010). Proteins provide a connection between the genetic information stored in DNA and how it is manifested in plant phenotypes. Methodological advances in protein analysis have led to the large-scale characterization of proteins involved in certain biological functions, within specific organs or tissues, at different developmental stages, or under environment stresses. Proteomics techniques are valuable tools for studying plant responses and possible resistance mechanisms. For example, a 2-DE-based protein separation method can be used to generate and compare profiles of global protein expression. One major advantage of this technique is that differentially expressed proteins can clearly and reproducibly be detected when infected and uninfected plants are examined. Proteins showing differential expression between treatments may have important roles in plant-stress responses. Being able to identify such proteins by MALDI technology provides insight into the molecular mechanisms of resistance as well as the underlying functions of those proteins in determining resistance by wheat plants (Kim et al., 2003; Ndimba et al., 2003; Wang et al., 2005).

In the proteomics study described here, our objective was to isolate proteins from a high-yielding Korean cultivar of wheat, 'Keumgang', that are induced soon after infection by *F. graminearum*. We employed MALDI-TOF/TOF mass spectrometry to characterize these differentially expressed proteins and help determine their involvement in pathogen resistance in wheat spikes.

Results and discussion

Fungal Invasion and Sporulation

Glumes in wheat are the floral bracts positioned in pairs at the pedestal of each spikelet (Esau, 1965). They partially enfold the two to five florets of a spikelet. In our experiment, we sprayed the spikes with a spore suspension of *F. graminearum* at 5 d after anthesis. Inoculated glumes were sampled at 12, 24, and 48 HAI. An additional sample was collected for SEM analysis immediately after inoculation. All SEM tissues were examined within 72 HAI (Fig. 1). The macroconidia germinated from the time of inoculation up to 48 HAI, on the abaxial side of the glumes. Hyphae showed immediate invasion and had frequent contact with the stomata, suggesting that these were the points of penetration. The first hyphae to emerge were uniformly thin and, initially, unbranched. After 12 HAI, we observed, via SEM, that the epidermal cells were directly penetrated by hyphae growing on the surface of the glumes, and the stomata were clearly visible. By 24 to 48 HAI, we saw that the hyphae were thickened and had very noticeable branching. These formations had a coralloid structure and were well-developed primarily along the stomatal rows. After 48 h, more thick hyphae were found in subcuticular locations. By that time point, conidiophores with developed macroconidia also were apparent on the glume surfaces, indicating that the fungus had quickly completed one asexual cycle on those tissues.

Fully developed hyphae with conidia were also observed at 24 and 48 HAI (Fig. 1). These results were similar to those previously reported with 'Sumai 3' and 'Wheatwon' (Pritsch et al., 2000). In addition, hyphae with predetermined conidia were clearly visible on the epidermal and subcuticular surfaces of the tissues at 48 and 76 HAI.

Proteomics Patterns in Wheat Spike Proteins Induced by F. graminearum

Changes in the *Fusarium*-induced proteome were monitored following inoculation. Proteins were isolated from control spikes as well as those collected at 12, 24, and 48 HAI. 2-DE separation was coupled with CBB-staining. Using image analysis by PDQuest software, we found more than 100 highly reproducible protein spots in each gel (Fig. 2). Of these, 31 (31%) could be classified as differentially expressed proteins (DEPs). They were broadly distributed, with p*I* values ranging from 3 to 10 and apparent molecular weights of between 10 and 250 kDa. By comparison, Wang et al. (2005) have used MALDI-TOF-MS with *Fusarium*-treated wheat spikes to describe 30 DEPs out of 1,104 protein spots, or 3.32%. Although our protein catalog was similar for both untreated and treated samples, many spots showed noticeable differences in protein abundance. Over the time course (12, 24, and 48 HAI), we categorized the profiles for 24 DEPs into three groups: up- (17 DEPs), down- (5), and unevenly regulated (2). This effect was more pronounced at 24 and 48 HAI. Under stress, 15 spots were altered by at least 2.34-fold compared with the control (Figs. 2, 3; Table 1).

FHB-responsive Protein Identified by MALDI-TOF/TOF MS

2-DE technology has been successfully applied for studying changes in protein patterns from spikes of wheat when induced by *F. graminearum* (Campo et al., 2004; Wang et al., 2005). However, while preparing our protein extracts, we encountered some problems associated with phenolic and nucleic acids, starch, and other contaminants. Nevertheless, the TCA protein precipitation method (Damerval et al., 1986; Porubleva et al., 2001; Kim et al., 2010) enabled us to overcome those challenges. Proteins from all 31 DEPs were subjected to tryptic digestion and analyzed by MALDI-TOF/TOF MS. Of the 24 DEPs identified here, most were plastid proteins. These were determined through MS fingerprint data and by querying the Swiss-Prot and NCBInr protein databases. Although some proteins could be matched with *Triticum* spp., most were matched with those from *Arabidopsis*, rice, barley, rye, and other cereals. This was because genome sequences are under-represented for wheat.
Photosynthetic enzymes dominated the 2-DE profile of leaf tissue, which is in agreement with reports for other plant species (Watson et al., 2003; Jorge et al., 2006; Castillejo et al., 2008). The majority of proteins identified here (70.8%) is related to photosynthesis, energy, and carbon metabolism (Table 2) .These include ribulose-1, 5-bisphosphate carboxylase (Spots 3, 11, 12, 18, and 23), Rubisco small subunits (3, 4, 11, 12, 14, 18, and 23), and Rubisco large subunits (8 and 16). Those that were up-regulated by stress included isoforms of Rubisco, a finding that agrees with that of Mahmood et al. (2006), who have examined bacterial leaf blight in rice blades. Interestingly, Spot #2 was down-regulated while Spot #14 was unevenly affected. Rubisco prompts both photosynthesis and carbon metabolism. During catalysis, it is first activated then carbanylated. Rubisco

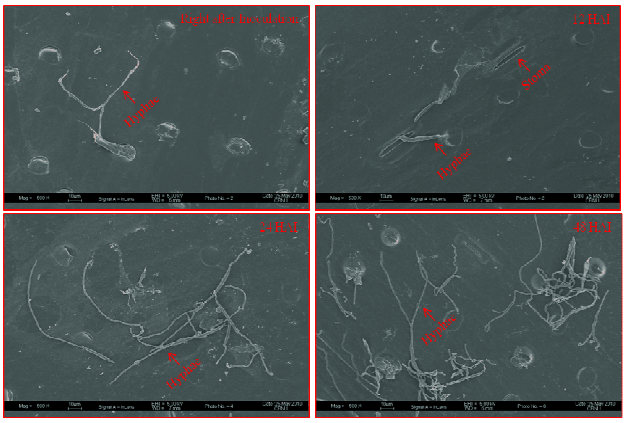

Fig 1. Early infection by *Fusarium graminearum* on axial surface of wheat glumes. Spikes were spray-inoculated with macroconidia suspension and sampled at 0, 12, 24, and 48 HAI for SEM analysis.

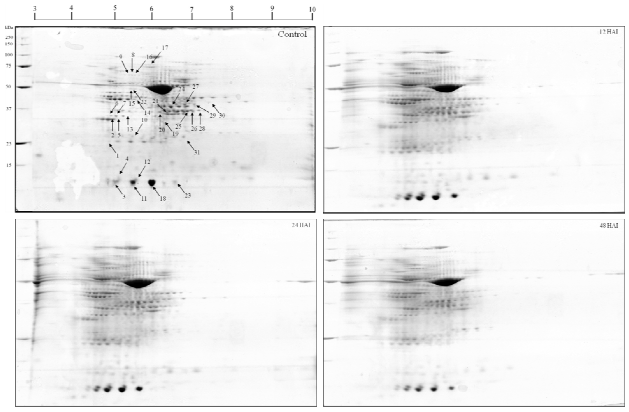

Fig 2. Effects of *Fusarium* head blight on protein expression in wheat spikes, based on comparisons among untreated control and spikes sampled at 12, 24, and 48 HAI. Proteins were extracted, separated by 2-DE, and visualized by CBB R-250 staining. The MW of each protein was determined by 2-DE markers. Arrows indicate proteins whose expression was changed by FHB infection, as measured with PDQuest image analyzer.

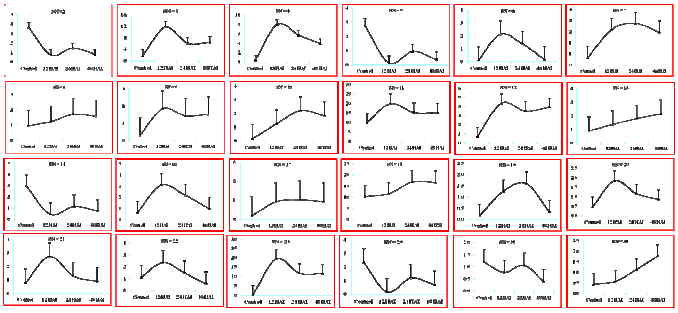

Fig 3. Relative protein abundance (%) from control (untreated) and inoculated spikes at 12, 24, or 48 HAI. Error bars indicate standard errors. Numbering of spots is same as for Figure 2 and Tables 1 and 2.

activase can alter that process by facilitating the dissociation of tightly bound sugar phosphates via ATP hydrolysis (Spreitzer and Savucci, 2002). Stress can cause both reversible and irreversible inactivation of Rubisco. However, this complementary enzyme releases those inhibitors of Rubisco, which is itself regulated by redox controls (Foyer and Parry, 2001). Rubisco activase is now the focus of research for improving the net rate of photosynthesis in crop species (Spreitzer and Savucci, 2002). In our study, oxygen-evolving enhancer protein 1 (Spots 2 and 5) an important component in Photosystem II, was down-regulated in treated wheat spikes; which is supported to over expression in rice by bacterial blight (Mahmood et al., 2009) (Figs. 2, 3; Tables 1, 2). Reactive oxygen species (ROS) are generated under biotic and abiotic stresses (Zou et al., 2005). Rice seedlings exposed to long-term abiotic stress, such as from high salt, the abundance of oxygen evolving enhancer protein 2 is decreased (Abbasi and Komatsu, 2004). OEE2 can be easily removed from the PSII complex in the presence of NaCl. Thus, increased levels of this protein might be needed to repair damage caused by dissociation and to maintain oxygen production (Gazanchian et al., 2007). Putative cytochrome C oxidase subunits (6, 9, 10, 13, 16, 17, and 19) were up-regulated by infection compared with the untreated samples. Cytochrome C oxidase, the terminal enzyme of the respiratory chain, oxidizes cytochrome *c* and transfers electrons to molecular oxygen, forming molecular water. It is induced by high salt, indicating its involvement in conferring tolerance to that stress (Yan et al., 2005) as well as resistance to blister rust in white pine (Smith et al., 2006). It can possibly facilitate energy generation through the respiratory chain under stress conditions. Wall-associated kinases (WAKs), which play a major role in controlling organ and tissue development, are expressed at organ junctions, in the apical meristems of shoots and roots, and in expanding leaves (Wagner and Kohorn, 2001). We observed that a protein from Spot #30, identified as a putative WAK, was markedly more abundant after induction by *F. graminearum*. This protein is also increased under Cu stress (Zhang et al., 2009). Functional analyses of different WAK gene members in *Arabidopsis* have demonstrated that they operate in pathogen resistance, aluminum tolerance, and mineral responses (He et al., 1998; Sivaguru et al., 2003; Hou et al., 2005). For example, Hou et al. (2005) have shown that although reduced expression of WAKL4 leads to hypersensitivity to Na, K, Cu, and Zn, its over-expression confers Ni tolerance. We identified an important plasma membrane protein (Spots 20 and 21), a chloride carrier/channel, that was up-regulated in treated spikes. All functionally characterized members of the Chloride Carrier (ClC) family are implicated in a voltage-regulated process. Those channels provide a variety of physiological roles, e.g., cell volume regulation, stabilization of membrane potential, signal transduction, and trans-epithelial transport (Worden et al., 2009). Nitrate is required for plant growth, and most is stored in the central vacuole. Some members of the ClC family, such as the torpedo-fish ClC-0 and mammalian ClC-1, are anion channels, whereas the *E. coli* EriC and mammalian ClC-4 and ClC-5 are Cl^-/H^+ exchangers. Several plant associates of the ClC family may be anion channels that function in nitrate homeostasis. However, *Arabidopsis thaliana* ClCa is localized to the tonoplast membrane of the plant vacuole (Bergsdorf et al., 2009), but is also able to accumulate nitrate in the vacuole, behaving as an NO_3^-/H^+ exchanger (de Angeli et al., 2006). In the cytoplasm, we identified isoflavone reductase homolog IRL, which was markedly up-regulated compared with the control. These results reflect those reported for soybean roots in response to *Fusarium solani* f. sp. Glycines (Iqbal et al., 2005) as well as participate in the restriction of pathogen invasion (Shadle et al., 2003). IRL may be involved in the synthesis of a non-thiol reducing agent that can act, either chemically or enzymatically, as an antioxidant protectant. A range of non-sulfur plant constituents, including flavonoids, a-tocopherols, ascorbic acid, and carotenoids, also guards against ROS and free radicals (lnzé and van Montagu, 1995). IRL expression is correlated closely with the availability of glutathione, being persistently induced in seedlings but down-regulated rapidly when levels of glutathione are restored. This glutathione-dependent regulation indicates that IRL may play a crucial role in the establishment of a thiol-independent response to oxidative stress when glutathione is depleted in maize (Petrucco et al., 1996). In our study, we identified (1,3;1,4) β-glucanase (EC 3.2.1.73; Spot #31), which was gradually increased, up to 4-fold, in treated spikes. This enzyme, which hydrolyzes 1,3;1,4-β-glucosidic linkages on 1,3;1,4-β-glucan, is an important component of cell walls. Transgenic plants spontaneously produce brown specks on their leaves, similar in appearance to those reported with an initiation type of disease-lesion-mimic mutants, and, occasionally, on older leaves even without pathogen inoculation. Expression of the related gene is drastically increased after the emergence of that lesion-mimic phenotype (Nishizawa et al., 2003). Additionally, 1, 3-β-glucanase (EC 3.2.1.39) is induced transcriptionally in many plants after infection by different types of pathogens, and is known to control a wide range of developmental processes (Simmons, 1994). Furthermore, 1,3;1,4 β-glucans, a major constituent of endosperm cell walls and, to a lesser degree, the cell walls of nearly all tissues in the Poaceae family, are thought to play an important role in vegetative growth (Gibeaut and Carpita, 1993). Whereas 1,3-β-glucanases have been demonstrated to function both in plant defenses and development, 1,3;1,4 β-glucanases have been studied most extensively with the growth of cereal plants. They have been shown to have key roles in endosperm degradation during kernel germination and in the elongation of vegetative cell walls (Simmons, 1994).

Materials and methods

Preparation of Macroconidia Inoculums

Fusarium graminearum Strain 6 (SCK-04) was cultured in the dark on potato dextrose agar (PDA) for 5 d at 25ºC. This macroconidial suspension was produced by transferring several PDA plugs (1 cm × 1 cm) from an established fungal culture onto 400 mL of carboxylmethylcellulose (CMC) broth (15 g of CMC, 1 g of yeast extract, 0.5 g of $MgSO_4 \cdot 7H_2O$, 1 g of NH_4NO_3, 1 g of KH_2PO_4, and 1 L of H_2O). This culture was incubated on a rotary shaker (150 rpm) at 24ºC for 9 to 13 d (McCallum and Tekauz, 2002; Geddes et al., 2008). Spores were counted on a hemacytometer.

Plant Growth and Artificial Inoculations

Field tests were conducted on the experimental grounds of Chungbuk National University, Cheong-ju, Chungbuk, South Korea. A Korean wheat cultivar, 'Keumgang', was selected as model plant because it is popular for making bread and noodles, and also shows moderate resistance to FHB. For

Table 2. Profiles for protein expression in response to *Fusarium* head blight, as identified via MALDI-TOF/TOF-MS.

SN	AN	Protein description	PS[1]	EMW	TMW	EPI	TPI	PM	PQ	PC	PS[2]
2	P12359	Oxygen-evolving enhancer protein 1, chloroplastic	258	31.2	35.4	4.51	5.58	2	55	30.2	GGSTGYDNAVALPAGGR
3	P07398	Ribulose bisphosphate carboxylase small chain clone 512	208	7.76	13.3	4.60	5.84	3	51	23.9	EHNASPGYYDGR
	gil207080698	Chloroplast ribulose-1,5-bisphosphate carboxylase/oxygenase small subunit	197		7.9		9.42	3	53	28.8	EHNASPGYYMGR
	P00871	Ribulose bisphosphate carboxylase small chain pws4.3, chloroplastic	157		19.7		8.99	3	53	15.5	EHNSSPGYYDGR
4	P07398	Ribulose bisphosphate carboxylase small chain clone 512	200	8.33	13.3	4.65	5.84	3	51	23.9	EHNASPGYYDGR
5	P12359	Oxygen-evolving enhancer protein 1, chloroplastic	228	31.3	35.4	4.61	5.58	2	68	20.2	DGIDYAAVTVQLPGGER
6	P84733	Putative cytochrome c oxidase subunit ii ps17	66	35.5	1.7	4.57	9.62	2	12	100	VVEALSPR
7	P52580	Isoflavone reductase homolog irl	105	35.3	32.8	4.66	5.69	2	58	26.5	FFPSEFGLDVDR
8	Q43831	Rubisco large subunit-binding protein subunit beta, chloroplastic	63	62.5	53.7	4.75	4.88	2	69	35.8	SSENNLYVVEGMQFER
9	P84733	Putative cytochrome c oxidase subunit ii ps17	65	62.5	1.7	4.68	9.62	2	11	100	VVEALSPR
10	P84733	Putative cytochrome c oxidase subunit ii ps17	67	24.8	1.7	4.81	9.62	2	7	100	VVEALSPR
11	P00871	Ribulose bisphosphate carboxylase small chain pws4.3, chloroplastic	202	7.75	19.7	4.87	8.99	3	46	15.5	EHNSSPGYYDGR
	gil207080698	Chloroplast ribulose-1,5-bisphosphate carboxylase/oxygenase small subunit	197		7.9		9.42	3	46	28.8	EHNASPGYYMGR
	P07398	Ribulose bisphosphate carboxylase small chain clone 512	274		13.3		5.84	4	44	31	EHNASPGYYDGR
12	gil207080698	Chloroplast ribulose-1,5-bisphosphate carboxylase/oxygenase small subunit	206	8.36	7.9	4.94	9.42	3	54	28.8	EHNASPGYYMGR
	P00871	Ribulose bisphosphate carboxylase small chain pws4.3, chloroplastic	156		19.7		8.99	3	54	15.5	EHNSSPGYYDGR
	P07398	Ribulose bisphosphate carboxylase small chain clone 512	241		13.3		5.84	4	52	31	EHNASPGYYDGR
13	P84733	Putative cytochrome c oxidase subunit ii ps17 1	62	35.1	1.7	4.87	9.62	2	9	100	VVEALSPR
14	Q7X999	Ribulose bisphosphate carboxylase/oxygenase activase 2, chloroplastic	66	40.8	48.3	4.94	6.78	2	66	45.1	GLAYDISDDQQDITR
16	Q43831	Rubisco large subunit-binding protein subunit beta, chloroplastic	72	62.7	53.7	4.83	4.88	2	74	25.8	SSENNLYVVEGMQFER
	P84733	Putative cytochrome c oxidase subunit ii ps17	67		1.7		9.62	2	9	100	VVEALSPR
17	P84733	Putative cytochrome c oxidase subunit ii ps17	80	64.2	1.7	5.01	9.62	2	11	100	VVEALSPR
18	gil207080698	Chloroplast ribulose-1,5-bisphosphate carboxylase/oxygenase small subunit	192	7.72	7.9	5.24	9.42	3	50	28.8	EHNASPGYYMGR
	P00871	Ribulose bisphosphate carboxylase small chain pws4.3, chloroplastic	151		19.7		8.99	3	50	15.5	EHNSSPGYYDGR
	P07398	Ribulose bisphosphate carboxylase small chain clone 512	248		13.3		5.84	4	47	31	EHNASPGYYDGR
19	P84733	Putative cytochrome c oxidase subunit ii ps17	68	33	1.7	5.33	9.62	2	9	100	VVEALSPR
20	gil226462786	Chloride carrier/channel family	54	36.2	69.9	5.23	5.84	2	6	29	IAPLSVTR
21	gil226462786	Chloride carrier/channel family	51	37.2	69.9	5.38	5.84	2	9	13	IAPLSVTR
22	gil255551479	Conserved hypothetical protein	41	42.8	8.2	5.13	10.89	2	4	12.1	AVAETVPR
23	gil207080698	Chloroplast ribulose-1,5-bisphosphate carboxylase/oxygenase small subunit	162	7.88	7.9	5.67	9.42	3	47	28.8	EHNASPGYYMGR
	P00871	Ribulose bisphosphate carboxylase small chain pws4.3, chloroplastic	123		19.7		8.99	3	47	15.5	EHNSSPGYYDGR
	P07398	Ribulose bisphosphate carboxylase small chain clone 512	208		13.3		5.84	4	45	31	EHNASPGYYDGR
29	gil37718901	Hypothetical protein	42	38	87.7	6.13	9.35	2	27	32.2	KSLSSPAISR
30	gil56784948	Wall-associated kinase 4-like	34	39.4	77.7	6.29	6.18	2	7	15.7	ALSWPLR
31	gil311764	(1,3;1,4) beta glucanase	51	27.7	35.0	6.31	6.5	2	69	19.2	LVVSESGWPSGGG TAATPANAR

Criteria: SN spot number; AN accession number; PS[1] protein score; EMW experimental molecular weight (kDa); TMW Theoretical molecular weight (kDa); EPI experimental p*I value; TPI theoretical* p*I value; PM peptide matches; PQ peptide queries; PC protein coverage (%); PS[2] peptide sequence*

pathogen inoculation, we collected spikes at 5 d after anthesis and quickly placed in test tubes filled with distilled water. Samples were prepared according to the cut-spike method (Han and Kim, 2005). After a freshly mixed conidial suspension (10 µL of 4.5×10^4 macroconidia mL^{-1}) was added to each tube, the spikes were transferred to a chamber (2 m × 2 m × 90 cm) that was covered with polythene. Growing conditions included a temperature of 25 to 26ºC and relative humidity of 60%. Three groups of five to six spikes each were collected at 12, 24, and 48 hours after inoculation (HAI). Control spikes were treated only by spraying them with water. All samples were immediately frozen in liquid nitrogen and stored at –80ºC prior to protein extraction, while those for SEM were used immediately.

Scanning Electron Microscopy (SEM)

Wheat glumes were cut into 0.5 × 0.5 mm segments. For primary fixation, the samples were held in 2.5%

glutaraldehyde and 0.1 M phosphate buffer (pH 7.4) for 3 to 4 h. Afterward, they were rinsed twice in phosphate buffer for 15 min each. Post-fixation, the samples were placed in 1% osmium tetroxide, and washed again for 15 min. They were then dehydrated with concentrated ethanol (30% and 100%; 10 min each). These tissues were preserved in isoamylacetate and air-dried. Afterward, they were pinned to aluminum stubs with conductive paint and coated with a gold palladium alloy in a Kinney (KSE-2A-M) vacuum evaporator. The abaxial face of the each glume was examined at 5 kV with a LEO 1530VP Ultra-high-resolution VP FE-SEM (LEO Electron Microscopy Ltd., Germany). Digital images were acquired with Leo 32 Image software by controlling the electron beam scanning raster by computer. Three glumes per sample per time point were examined in combination before the best visualized image was selected according to a method modified from that of Pritsch et al. (2000).

Protein Extraction and Gel Electrophoresis

From control and inoculated spikes, we prepared proteins for IEF according to a modified version of the trichloroacetic acid (TCA)/acetone method (Damerval et al., 1986; Porubleva et al., 2001; Kim et al., 2010). Each 200 µL of sample was suspended in a 1:4 (sample:extraction buffer) volume of TCA solution (10% TCA/acetone solution containing 0.07% 2-mercaptoethanol plus a 0.04% protease inhibitor cocktail for plant cell and tissue extracts). After vortexing, the solution was frozen at –20°C for 1 h, then centrifuged at 14,000×*g* for 30 min. The precipitate was suspended in wash buffer (acetone containing 0.07% 2-mercaptoethanol plus 0.04% protease inhibitor cocktail). After standing for 12 h at –20°C, the suspension was centrifuged at 14,000×*g* for 30 min. Afterward, the precipitate was dried *in vacuo*, and a part of the resultant powder was suspended in 500 µL of sample lysis buffer [6 M urea, 2 M thio-urea, 10 mM Tris-HCl, 0.75% ampholine (pH 3 to 10), 50 mM DTT, 4% CHAPS, and 0.4% protease inhibitor cocktail]. After incubating at room temperature for 2 h with continuous vortexing, the suspension was centrifuged at 14,000×*g* for 30 min and the resulting supernatant was subjected to IEF. Protein concentrations in the sample were determined by the method of Bradford (1976), using a Bio-Rad protein assay kit (Bio-Rad, Hercules, CA, USA) and bovine serum albumin (BSA) as the standard. Soluble proteins that are active under stress were examined by 2-DE according to the protocol of O'Farrell (1975). For the first dimension, sample solutions (400 µg) were loaded on the acidic side of the IEF tube gels. To avoid overlap by the protein spots and to increase the resolution capacity, we utilized an IEF gel specific for a pH range of 3 to 10 in addition to those for acidic and basic pH values. SDS-PAGE in the second dimension (Nihon Eido, Tokyo, Japan) was performed with 12% separation and 5% stacking gels. Protein spots on the 2-DE gels were visualized by staining with Coomassie Brilliant Blue (CBB R-250). Each sample was run five times, and the best triplicate visualized gels were selected for image analysis.

Gel Image Analysis

All gel images were captured with a flatbed scanner (HP Scanjet G4010; USA; 300 dpi, 32 bits per pixel). Computer-assisted 2-DE image analysis was evaluated with PDQuest software (Version 7.1; Bio-Rad). Isoelectric point (p*I*) and molecular weight (MW) of each protein were determined by 2-DE markers (Bio-Rad). The amount covered by a protein spot was expressed as the volume of that spot, defined as the sum of the intensities of all pixels that made up the spot. To correct for variability due to CBB-staining and to reflect any quantitative variations in intensities, the spot volumes were normalized as a percentage of the total volume in all spots present on the gel. Three biological replications were used; spots that were up- or down-regulated in at least two biological replications were considered reproducibly regulated. Statistical analysis of the data was carried out with Microsoft Excel 2007, and the standard error (SE) was calculated from three spots on separate gels.

In-gel Digestion and MALDI-TOF/TOF-MS Analysis

Protein spots were manually excised from the 2-DE gel, and in-gel digestion by trypsin was performed as described by Kim et al. (2005). Briefly, CBB-stained gel pieces were washed several times with water and then with 30% methanol before being de-stained with 10 mM NH_4CO_3 in 50% ACN. Proteins were reduced with 10 mM DTT in 100 mM NH_4CO_3 at 56°C for 1 h, then alkylated with 55 mM IAA (iodoacetamide) in 100 mM NH_4CO_3 in the dark for 40 min. The gel pieces were minced, lypolized, and re-hydrated overnight at 37°C in 50 mM NH_4CO_3 with 11.9 ng μL^{-1} of sequencing-grade-modified trypsin (Promega Corp.). After tryptic digestion, the peptides were extracted four times with a solution containing 0.1% formic acid in 50% ACN. That solution was concentrated to dryness under a vacuum. Peptides that had been digested by trypsin were dissolved in 0.5% (v/v) trifluoroacetic acid (TFA) and de-salted with a ZipTip C_{18} (Millipore, Bedford, MA, USA). Those purified peptides were then eluted directly onto a MALDI plate by using α-cyano-4-hydroxy-cinnamic acid (CHCA) matrix solution [10 mg mL^{-1} of CHCA in 0.5% (v/v) TFA/50% (v/v) acetonitrile; 1:1]. All mass spectra were acquired in the reflection mode by a 4700 Proteomics Analyzer (Applied Bio-Systems, Framingham, MA, USA). External calibration was performed with a standard peptide mixture of des-Arg bradykinin, angiotensin, Glu-fibrinopeptide B, adrenocorticotropic hormone (ACTH) clip 1-17, ACTH clip 18-39, and ACTH clip 7-38.

Bioinformatics

Our acquired MS/MS spectra were evaluated with an in-house licensed search engine (Mascot Version 2.3.01; Matrix Science, London, England, UK) against the viridiplantae (green plants) within the UNIPROT_SPROT and NCBInr databases. The carbamidomethylation of cysteines was set as a fixed modification while the oxidation of methionines was set as a variable modification. Trypsin was specified as the proteolytic enzyme and one missed cleavage was allowed. Mass tolerance of the precursor ion was 25 ppm; that of the fragment ions, 0.5 Da. The instrument setting was specified as 'MALDI-TOF/TOF'. Protein hits were validated if the identification involved at least 10 top-ranking peptides with p-values ≤0.05 and peptide scores >34. When those peptides matched multiple members of a protein family, the presented protein was selected based on the highest score and the greatest number of matching peptides. For functional categorization based on gene ontology, we utilized the Protein Information Resources, or PIR (http://pir.georgetown.edu). This integrated public bioinformatics source supports genomics, proteomics, and systems biology research. It is used for determining gene ontology-based molecular functions, cellular components, and biological processes,

which are then automatically classified in the data set according to biological process per Batch Retrieval with the *i*ProClass database (Huang et al., 2003).

Conclusion

By using SEM and proteomics techniques, we have identified several proteins associated with the response by wheat spikes to *Fusarium* inoculation. They present differential changes in abundance over a time-dependent course of infection. Most are related to the plastids, especially chloroplasts, which are involved in carbon metabolism and photosynthesis. Our results indicate that plastids, plasma membranes, and kinase-like proteins show defense responses following infection. Therefore, we suggest that proteome studies with 2-DE provide valuable tools for identifying the acidic and basic proteins that respond to this fungus, as well as for better understanding their interactive effect in conferring pathogen resistance. This will be beneficial for future FHB research when using marker-assisted selection and gene transfer technology.

Acknowledgements

Financial support for this study was obtained from the AGENDA (20090101036022), RDA, Korea to S. H. Woo, and partially funded by the Korea Basic Science Institute Grant (G30121) to Cho Kun and K-Mep Project (T30110) of Korea Basic Science Institute to J. S. Choi.

References

Abbasi FM, Komatsu S (2004) A proteomic approach to analyze salt-responsive proteins in rice leaf sheath. Proteomics 4:2072-2081

Bai GH, Shaner G (2004) Management and resistance in wheat and barley to *Fusarium* head blight. Annu Rev Phytopathol 42:135-161

Bergsdorf EY, Zdebik AA, Jentsch TJ (2009) Residues important for nitrate/proton coupling in plant and mammalian CLC transporters. J Biol Chem 284:11184-11193

Bradford M (1976) A rapid and sensitive method for the quantitation of microgram quantities of protein utilizing the principle of protein-dye binding. Anal Biochem 72:248-254

Campo S, Carrascal M, Coca M, Abian J, San Segundo B (2004) The defense response of germinating maize embryos against fungal infection: a proteomics approach. Proteomics 4:383-396

Castillejo MA, Maldonado AM, Ogueta S, Jorr´ın JV (2008) Proteomic analysis of responses to drought stress in sunflower (*Helianthus annuus*) leaves by 2DE gel electrophoresis and mass spectrometry. Open Proteomics J 1:59-71

Damerval C, de Vienne D, Zivy M, Thiellement H (1986) Technical improvements in two-dimensional electrophoresis increase the level of genetic variation detected in wheat-seedling proteins. Electrophoresis 7:52-54

de Angeli A, Monachello D, Ephritikhine G, Frachisse JM, Thomine S, Gambale F, Barbier-Brygoo H (2006) The nitrate/proton antiporter AtCLCa mediates nitrate accumulation in plant vacuoles. Nature 442:939-942

Desjardins AE, Hohn TM (1997) Mycotoxins in plant pathogenesis. Mol Plant Microbe Interact 10:147-152

Esau K (1965) The flower. Plant Anatomy, Wiley and Sons, New York

Foyer CH, Parry MAJ (2001) Green shoots of sustainability plant responses to stress. Institute of Arable Crops Research Report pp 16-19

Gazanchian A, Hajheidari M, Sima NK, Salekdeh GH (2007) Proteome response of *Elymus elongatum* to severe water stress and recovery. J Exp Bot 58:291-300

Geddes J, Eudes F, Laroche A, Selinger LB (2008) Differential expression of proteins in response to the interaction between the pathogen *Fusarium graminearum* and its host, *Hordeum vulgare*. Proteomics 8:545-554

Gibeaut DM, Carpita NC (1993) Synthesis of (1-3),(1-4)-β-D-glucan in the golgi apparatus of maize coleoptiles. Proc Natl Acad Sci USA 90:3850-3854

Han OK, Kim JK (2005) Establishment of artificial screening methods and evaluation of barley germplasms for resistance to *Fusarium* head blight. Korean J Crop Sci 50:191-196

He ZH, He D, Kohom BD (1998) Requirement for the induced expression of a cell wall associated receptor kinase for survival during the pathogen response. Plant J 14:55-63

Hou XM, Tong HY, Selby J, DeWitt J, Peng XX, He ZH (2005) Involvement of a cell wall-associated kinase, WAKL4, in Arabidopsis mineral responses. Plant Physiol 139:1704-1716

Huang H, Barker WC, Chen Y, Wu CH (2003) *i*ProClass: an integrated database of protein family, function and structure information. Nucl Acids Res 31:390-392

Inzé DD, Van Montagu M (1995) Oxidative stress in plants. Curr Opin Biotechnol 6:153-158

Iqbal MJ, Yaegashi S, Ahsan R, Shopinski KL, Lightfoot DA (2005) Root response to *Fusarium solani* f. sp . *glycines*: temporal accumulation of transcripts in partially resistant and susceptible soybean. Theor Appl Genet 110:1429-1438

Jorge I, Navarro R.M, Lenz C, Ariza D, Jorr´ın JV (2006) Variation in the holm oak leaf proteome at different plant developmental stages, between provenances and in response to drought stress. Proteomics 6:S207–S214

Kang Z, Buchenauer H (1999) Immunocytochemical localization of Fusarium toxins in infected wheat spikes by *Fusarium culmorum*. Physiol Mol Plant Pathol 55:275-288

Kim JY, Lee JH, Park GW, Cho K, Kwon KH, Park YM, Cho SY, Paik YK, Yoo JS (2005) Utility of electrophoretically derived protein mass estimates as additional constraints in proteome analysis of human serum based on MS/MS analysis. Proteomics 5: 3376-3385

Kim KH, Kamal AHM, Shin KH, Choi JS, Heo HY, Woo SH (2010) Large-scale proteome investigation in wild relatives (A, B and D genomes) of wheat. Acta Biochim et Biophys Sin 42: 709-716

Kim ST, Cho KS, Yu S, Kim SG, Hong JC, Han CD, Bae DW, Nam MH, Kang KY (2003) Proteomic analysis of differentially expressed proteins induced by rice blast fungus and elicitor in suspension-cultured rice cells. Proteomics 3:2368-2378

Kruger WM, Pritsch C, Chao S, Muehlbauer GJ (2002) Functional and comparative bioinformatic analysis of expressed genes from wheat spikes infected with *Fusarium graminearum*. Mol Plant Microbe Interact 15:445-55

Lin F, Kong ZX, Zhu HL, Xue SL, Wu JZ, Tian DG, Wei JB, Zhang CQ, Ma ZQ (2004) Mapping QTL associated with resistance to *Fusarium* head blight in the Nanda2419 × Wangshuibai population. I. Type II resistance. Theor Appl Genet 109:1504-1511

Mahalingam R, Gomez-Buitrago A, Eckardt N, Shah N, Guevara-Garcia A, Day P, Raina R, Fedoroff NV (2003) Characterizing the stress/defense transcriptome of *Arabidopsis*. Genome Biol 4:R20

Mahmood T, Jan A, Kakishima M, Komatsu S (2006) Proteomic analysis of bacterial-blight defense responsive proteins in rice leaf blades. Proteomics 6:6053-6065

Mahmood T, Jan A, Komatsu S (2009) Proteomic analysis of bacterial blight defense signaling pathway using transgenic rice over expressing thaumatin-like protein. Biol Plant 53:285-293

Martin RA, Johnston HW (1982) Effects and control of *Fusarium* diseases of cereal grains in the Atlantic Provinces. Can J Plant Pathol 4:210-216

McCallum BB, Tekauz A (2002) Influence of inoculation method and growth stage on *Fusarium* head blight in barley. Can J Plant Pathol 24:77-80

McMullen M, Jones R, Gallenburg D (1997) Scab of wheat and barley: a re-emerging disease of devastating impact. Plant Dis 81:1340-1348

Mesterházy Á (1997) Methodology of resistance testing and breeding against *Fusarium* head blight in wheat and results of the selection. Cereal Res Comm 25:631-637

Ndimba BK, Chivasa S, Hamilton JM, Simon WJ, Slabas AR (2003) Proteomic analysis of changes in the extracellular matrix of Arabidopsis cell suspension cultures induced by fungal elicitors. Proteomics 3:1047-1059

Nishizawa Y, Saruta M, Nakazono K, Nishio Z, Soma M, Yoshida T, Nakajima E, Hibi T (2003) Characterization of transgenic rice plants over-expressing the stress-inducible *β*-glucanase gene *Gns1*. Plant Mol Biol 51:143-152

O`Farrell PH (1975) High resolution two-dimensional electrophoresis of proteins. J Biol Chem 250: 4007-4021

Petrucco S, Bolchi A, Foroni C, Percudani R, Rossi GL, Ottonello S (1996) A maize' gene encoding an nadph binding enzyme highly homologous to lsoflavone reductases is activated in response to sulfur starvation. Plant Cell 8:69-80

Porubleva L, Velden KV, Kothari S, Oliver DJ, Chitnis PR (2001) The proteome of maize leaves: use of gene sequences and expressed sequence tag data for identification of proteins with peptide mass fingerprints. Electrophoresis 22:1724-1738

Pritsch C, Muehlbauer GJ, Bushnell WR, Somers DA, Vance CP (2000) Fungal development and induction of defense response genes during early infection of wheat spikes by *Fusarium graminearum*. Mol Plant Microbe Interact 13:159-169

Shadle GL, Wesley SV, Korth KL, Chen F, Lamb C, Dixon RA (2003) Phenylpropanoid compounds and disease resistance in transgenic tobacco with altered expression of L-phenylalanine ammonia-lyase. Phytochem 64:153-161

Shifrin VI, Anderson P (1999) Trichothecene mycotoxins trigger a ribotoxic stress response that activates c-Jun N-terminal kinase and p38 mitogen-activated protein kinase and induces apoptosis. J Biol Chem 274:13985-13992

Simmons CR (1994) The physiology and molecular biology of plant 1,3-*β*-D-glucanases and 1,3;1,4-*β*-D-glucanases. Crit Rev Plant Sci 13:325-387

Sivaguru M, Ezaki B, He ZH, Tong H, Osawa H, Baluska F, Volkmann D, Matsumoto H (2003) Aluminum-induced gene expression and protein localization of a cell wall-associated receptor kinase in *Arabidopsis*. Plant Physiol 132:2256-2266

Smith JA, Blanchette RA, Burnes TA, Jacobs JJ, Higgins L, Witthuhn BA, David AJ, Gillman JH (2006) Proteomic comparison of needles from blister rust-resistant and susceptible *Pinus strobus* seedlings reveals up-regulation of putative disease resistance proteins. Mol Plant Microbe Interact 19:150-60

Spreitzer RJ, Savucci ME (2002) Rubisco: structure, regulatory interactions and possibilities for a better enzyme. Annu Rev Plant Biol 53:449-485

Taylor RD, Saparno A, Blackwell B, Anoop V, Gleddie S, Tinker NA, Harris LJ (2008) Proteomic analyses of *Fusarium graminearum* grown under mycotoxin-inducing conditions. Proteomics 8:2256-2265

van Eeuwijk FA, Mesterhazy A, Kling CI, Ruckenbauer P, Saur L, Buerstmayr H, Lemmens M, Keizer LCP, Maurin N, Snijders CHA (1995) Assessing non-specificity of resistance of wheat to head blight caused by inoculation with European strains of *Fusarium culmorum*, *F. graminearum* and *F. nivale*, using a multiplicative model for interaction. Theor Appl Genet 90:221-228

Wagner TA, Kohorn BD (2001) Wall-associated kinases are expressed throughout plant development and are required for cell expansion. Plant Cell 13:303-318

Walter S, Nicholson P, Doohan FM (2010) Action and reaction of host and pathogen during Fusarium head blight disease. New Phytol 185:54-66

Wang Y, Yang L, Xu H, Li Q, Ma Z, Chu C (2005) Differential proteomic analysis of proteins in wheat spikes induced by *Fusarium graminearum*. Proteomics 5:4496-4503

Watson BS, Asirvatham VS, Wang L, Summer LW (2003) Mapping the proteome of barrel medic (*Medicago truncatula*). Plant Physiol 131:1104-1123

Worden AZ, Lee JH, Mock T (2009) Green evolution and dynamic adaptations revealed by genomes of the marine picoeukaryotes *Micromonas*. Science 324:268-272

Yan S, Tang Z, Su W, Sun W (2005) Proteomic analysis of salt stress-responsive proteins in rice root. Proteomics 5:235-244

Zhang H, Lian C, Shen Z (2009) Proteomic identification of small, copper-responsive in germinating embryos of *Oryza sativa*. Ann Bot 103:923-930

Zou J, Rodriguez-Zas S, Aldea M, Li M, Zhu J, Gonzalez DO, Vodkin LO, DeLucia E, Clough SJ (2005) Expression profiling soybean response to *Pseudomonas syringae* reveals new defense-related genes and rapid HR-specific down-regulation of photosynthesis. Mol Plant-Microbe Interact 18:1161-1174